

VYSOKÉ UČENÍ TECHNICKÉ V BRNĚ  
BRNO UNIVERSITY OF TECHNOLOGY



FAKULTA STROJNÍHO INŽENÝRSTVÍ  
ÚSTAV MATEMATIKY

FACULTY OF MECHANICAL ENGINEERING  
INSTITUTE OF MATHEMATICS

# CFD MODELOVÁNÍ HOŘENÍ TUHÝCH PALIV NA ROŠTU

CFD MODELLING OF GRATE COMBUSTION OF SOLID FUELS

DIPLOMOVÁ PRÁCE  
DIPLOMA THESIS

AUTOR PRÁCE  
AUTHOR

TOMÁŠ JUŘENA

VEDOUcí PRÁCE  
SUPERVISOR

doc. Ing. JIŘÍ HÁJEK, Ph.D.

BRNO 2008

## **Abstrakt**

Práce je zaměřena na vytvoření numerického modelu 1D experimentálního reaktoru pro spalování tuhých paliv. Metodou konečných objemů je provedena diskretizace řídicích rovnic a takto formulovaná úloha je implementována do programu v prostředí MATLAB. V závěru jsou uvedeny výsledky několika simulací hoření slámy.

## **Summary**

The thesis is focused on numerical model development of one-dimensional experimental reactor for combustion of solid fuels. The finite volume method is used for discretizing the governing equations and the resulting formulation is implemented in the MATLAB code. Some illustrative simulation results of straw combustion are included as well.

## **Klíčová slova**

metoda konečných objemů, numerický model, biomasa, spalování biomasy na roštu, pevné lože

## **Keywords**

finite volume method, numerical model, biomass, grate combustion of biomass, fixed bed

JUŘENA, T. *CFD modelování hoření tuhých paliv na roštu*. Brno: Vysoké učení technické v Brně, Fakulta strojního inženýrství, 2008. 38 s. Vedoucí diplomové práce doc. Ing. Jiří Hájek, Ph.D.

Prohlašuji, že jsem diplomovou práci *CFD modelování hoření tuhých paliv na roštu* vypracoval samostatně pod vedením doc. Ing. Jiřího Hájka, Ph.D., s použitím materiálů uvedených v seznamu literatury.

Tomáš Juřena

Rád bych poděkoval panu doc. Ing. Jiřímu Hájkovi, Ph.D. za odborné vedení při práci, nesčetné hodiny, které mi věnoval při konzultacích a za pomoc při závěrečném ladění výsledného programu. Také bych chtěl poděkovat rodičům a blízkým za jejich veškerou podporu během studia.

Tomáš Juřena

# Contents

<b>1</b>	<b>Introduction</b>	<b>3</b>
1.1	State of the art . . . . .	3
1.2	Significance of 1-D models . . . . .	4
1.3	Objectives of the thesis . . . . .	4
1.4	Scope of the thesis . . . . .	4
<b>2</b>	<b>Mathematical model</b>	<b>5</b>
2.1	Physical model . . . . .	5
2.2	Main assumptions . . . . .	5
2.3	Combustion processes . . . . .	7
2.3.1	Moisture evaporation . . . . .	7
2.3.2	Devolatilization . . . . .	7
2.3.3	Char oxidation . . . . .	8
2.4	Governing equations . . . . .	10
2.4.1	Solid phase PDE's . . . . .	10
2.4.2	Gas phase PDE's . . . . .	12
2.5	Initial and boundary conditions . . . . .	14
2.5.1	Initial conditions . . . . .	14
2.5.2	Boundary conditions . . . . .	15
2.6	Summary . . . . .	15
<b>3</b>	<b>Numerical model</b>	<b>16</b>
3.1	Selection of the method . . . . .	16
3.2	Discretization . . . . .	16
3.2.1	General transport equation . . . . .	17
3.2.2	Spatial discretization . . . . .	17
3.2.3	Temporal discretization . . . . .	19
3.2.4	Final discretization equation . . . . .	19
3.2.5	Boundary conditions . . . . .	21
3.3	Iterative procedure . . . . .	22
3.4	Application to the system of PDE's . . . . .	22
3.4.1	Solid phase . . . . .	22
3.4.2	Gas phase . . . . .	24
3.5	Overall algorithm . . . . .	26
3.6	Program implementation . . . . .	26
3.6.1	Data and M-file organization . . . . .	26
3.6.2	Program tuning and simulation results . . . . .	28

3.7 Summary . . . . .	32
<b>4 Conclusion and future work</b>	<b>34</b>

# Chapter 1

## Introduction

Computational Fluid Dynamics (CFD) stands in the foreground of present-day methods for analysis and solution-finding of engineering problems that involve fluid flows. It has become the main tool of predicting flow fields, chemical driven processes as well as investigating and eliminating the causes of undesirable process behaviour, optimizing technologies, etc., [1]. Of course, the list of branches where CFD is being utilized is much longer than this. In spite of this, it is important to stress that CFD computer programs are able to solve only a limited set of problems, while the rest of problems must be adapted to the scope of the solver in a way (e.g. by stating some additional assumptions), or solved by another tool.

However, advanced softwares like Fluent provide to users a way of handling such situations by attaching their own source codes to the solver. Via the so called user defined functions (UDF) one can extend standard solvers by setting up some special conditions, procedures, functions, etc. in his own (for instance) C-programming language source code and upload it into the existing model, see [2].

### 1.1 State of the art

Modelling of grate combustion as a basic technology of heat production by burning fuels is not possible with commercial CFD code only. It is possible to solve gas phase processes above the fuel, but both physical and chemical processes occurring inside the fuel bed cannot be modeled using the CFD code itself. A stand-alone computer program solving the interactions between the solid and gas phases during combustion in the bed must be developed to carry out simulation of the processes. For further development of a grate furnace such a program is used in conjunction with a CFD program. The bed model determines the gas phase boundary conditions for the CFD model which can predict processes in the furnace.

A large model of this kind with moving bed has successfully been developed by Kær [3]. The model presented there considers the bed as a number of three dimensional volumes, each of which is considered not to exchange heat with other volumes through the side walls. Thus the heat transfer can be modeled as one-dimensional problem. Also a lot of work has been done on description of gas phase reactions and turbulence [4].

The work on detailed description of fixed bed biomass combustion so far has been focused on straw [5], [6], [7], [8]. Their theoretical results obtained from computer simulations and parametric studies indicate that the effective heat conductivity, straw packing

conditions, and heat capacity of the straw have considerable effects on the model predictions of such combustion. These conclusions also have been confirmed by experimental measurements.

## **1.2 Significance of 1-D models**

It has already been mentioned that theoretical results are compared with experimental ones. Development of industrial furnaces is based on results from 2-D or 3-D simulations. Such simulations require high quality of input data, mainly the packing conditions which are expressed in terms of the bed porosity and its effects on the flow, detailed description of convection/conduction and radiation mechanisms via the effective thermal conductivity, and the contents of moisture, char, volatiles, and ash in biomass which influence the effective heat capacity of the fuel [6].

Since data are better collected and evaluated from small-scaled laboratory reactors, the research is focused on 1-D modeling of processes in the mentioned experimental reactors. The results help in getting an insight into the mechanisms governing the combustion, and can be used in further development of higher-dimensional models.

## **1.3 Objectives of the thesis**

This thesis is aimed at constructing a numerical model simulating grate combustion of solid fuels in a one-dimensional experimental reactor. It is not intended to write the UDF for Fluent in this stage. The program should verify the mathematical model and thus serve for validation of the theoretical description approach and empirical parameters.

## **1.4 Scope of the thesis**

Physical and mathematical models are presented in the second section. The mathematical model includes the description of particular processes that are considered in combustion, i.e. moisture evaporation, devolatilization, and char oxidation. Then the interaction between gas and solid phases is described by a system of temperature-coupled partial differential equations where the process rate parameters and other physical quantities obtained from the three processes mentioned before play an important role.

A numerical method for solving the governing equations is discussed in the third section. The solution algorithm is proposed and results from computer simulation are shown. The work is concluded by a paragraph where suggestions for future work are stated.



# Chapter 2

## Mathematical model

The main purpose of this thesis is to verify the mathematical model of grate combustion which has been described in detail in [9]. Although this model is valid for any kind of solid fuels, the description of combustion processes is aimed at straw combustion due to the best data availability. For detailed mathematical description of the problem the physical model is briefly outlined first.

### 2.1 Physical model

Figure 2.1 shows a schematic diagram of an experimental furnace with a fixed bed. It is a vertical thick cylinder that consists of an air preheating section at the bottom, fuel bed combustion chamber and a secondary combustion chamber where gases from the primary chamber burn out. An electrical heater placed on the top of the bed serves as the source of radiation heat flux for heating and ignition of the fuel. The air is supplied from the bottom and is preheated to a certain temperature. Then it enters the bed consisting of small pieces of cut straw, and flows upward. Gas samples are collected from just above the top of the bed. On the other hand, the ignition starts at the top of the bed and the flame front travels the opposite direction. There are several thermocouples along the bed to measure the bed temperatures at different heights and both the primary air and flue gas temperatures.

### 2.2 Main assumptions

Mathematical description of a problem begins with stating all assumptions. These assumptions usually simplify the model in a sense, but at the same time they should reflect behaviour of the real system being modeled.

The furnace is relatively high with respect to its other dimensions. The air passes through an air preheating section into the fuel bed with a grate at the bottom. The bed is stationary when the primary air-flow rate is less than  $0,3 \text{ kg} \cdot \text{m}^{-2} \cdot \text{s}^{-1}$  [6]. The gas is supposed to be ideal and it is in plug-flow. Due to this facts, the system can be mathematically described as one-dimensional. The gas pressure is assumed constant. Also the combustion chamber is supposed to be adiabatic, i.e. no heat loss along the bed wall occurs during the combustion.

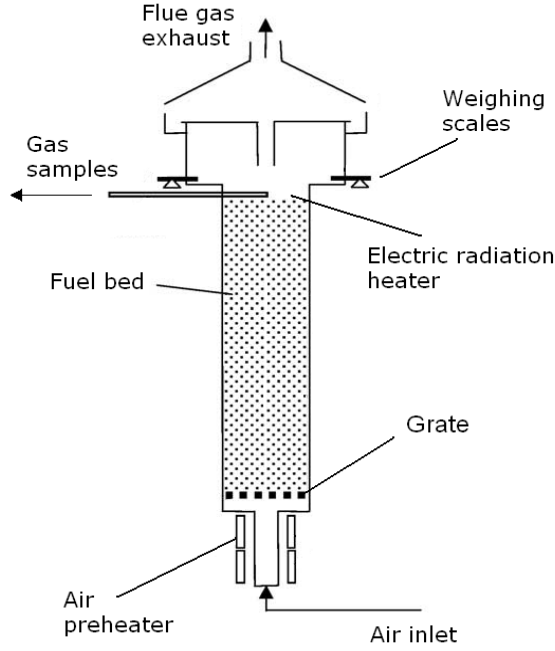


Figure 2.1: Experimental furnace

According to [6], bed volume reduction during combustion can be neglected. The gas-phase species included in the model are  $\text{CO}$ ,  $\text{CO}_2$ ,  $\text{H}_2\text{O}$ ,  $\text{O}_2$ ,  $\text{H}_2$ ,  $\text{N}_2$  and a single compound  $\text{C}_x\text{H}_y$  representing higher hydrocarbons. Some research teams distinguish several hydrocarbons, namely methane ( $\text{CH}_4$ ), higher hydrocarbons represented by an artificial substitute  $\text{C}_x\text{H}_y$  and tar (which is a complex mixture of condensable hydrocarbons [6]) and model them as independent gas-phase species, too. For the purpose of the thesis, it is sufficient to represent the hydrocarbons by an arbitrary compound, namely  $\text{C}_2\text{H}_6$ . Gas phase reactions are not included in the model, so physically, the ethane participates only in overall mass balance and carries some sensible heat.

The char remaining in the fuel and all combustible gas-phase species react with  $\text{O}_2$ . The rates of oxidation depend on the temperature. Although oxidation in the gas phase becomes very significant when the temperature is high (above 1000 K [5]), the model presented here does not take it into account (assuming that combustion of volatiles takes place only above the fuel layer). The only reaction with  $\text{O}_2$  is oxidation of char (solid-state carbon) fixed in the solid residual.

The following enumeration sums up all assumptions that have been stated.

- The system is one-dimensional, the gas is ideal and in plug-flow, its pressure is constant, and the combustion chamber is assumed to be adiabatic.
- The bed is stationary, there are no changes of packing conditions (volume reduction) during the process.
- Gas-phase species included in the model:  $\text{CO}$ ,  $\text{CO}_2$ ,  $\text{H}_2\text{O}$ ,  $\text{O}_2$ ,  $\text{H}_2$ ,  $\text{N}_2$ ,  $\text{C}_2\text{H}_6$ .

- Oxidation of char fixed in the solid residual is the only reaction with  $O_2$ .

Note that this list includes only the most important assumptions, whereas many others are implicit to the details of process rate models (e.g. shape and dimensions of fuel particles, overall properties of the fuel bed like thermal conductivity, physical properties of the gases like specific heat, etc.).

## 2.3 Combustion processes

The combustion of biomass is a combination of several processes. These sub-processes include evaporation of moisture from the fuel, devolatilization, burning of the volatiles, and the oxidation of char particles. However, combustion of the volatiles (gas products of devolatilization process) is assumed to take place only above the fuel bed, i.e. outside of the modelled domain. The description of the modelled processes via process rate equations is provided in the following. All equations in this section are taken from [6] for the sake of consistency, but alternative expressions and constants published by other authors are mentioned throughout the text. Note that the model has been designed for straw combustion.

### 2.3.1 Moisture evaporation

Biomass contains moisture as liquid water stored in the pores due to capillary forces and water bound to the biomass structure by intra-molecular forces. The volumetric rate of moisture release (due to fuel drying) is determined by

$$r_{H_2O} = k_d S (C_{w,s} - C_{w,f}), \quad (2.3.1)$$

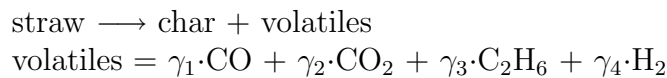
where  $k_d$  is the mass transfer coefficient,  $C_{w,s}$  and  $C_{w,f}$  are the concentrations of moisture at the straw surface and in the gas flow, respectively, and

$$S = \frac{2\rho_s r_{ext}}{\rho_{straw}(r_{ext}^2 - r_{in}^2)} \quad (2.3.2)$$

is the particle surface area per unit volume. Here,  $r_{ext}$  and  $r_{in}$  is external and internal radius of the straw, respectively, and  $\rho_s$ ,  $\rho_{straw}$  is the bulk density of straw and the density of straw wall, respectively. These densities are defined more precisely in the following.

### 2.3.2 Devolatilization

After moisture evaporation, the dried fuel is pyrolysed (devolatilised). Fuel consists of moisture, volatiles, char, and ash. Typical fuel composition is shown in the figure 2.2. The devolatilization (pyrolysis) can be described by the following scheme (adapted from [6]):



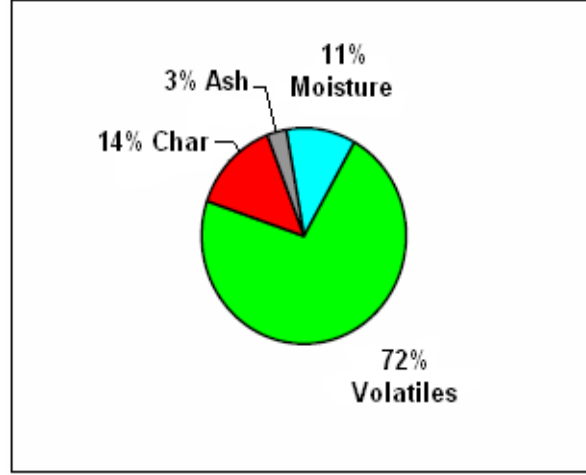


Figure 2.2: Example of fuel composition (straw)

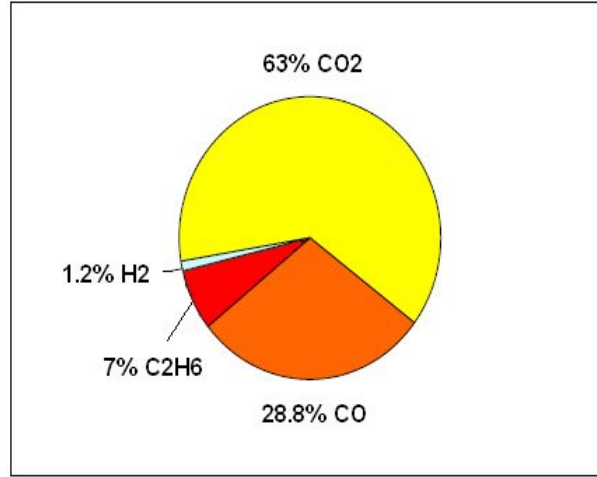


Figure 2.3: Yields of pyrolysis of dry straw

Coefficients  $\gamma_i$  represent mass fractions of different species formed during pyrolysis. Yields of pyrolysis products of dry straw are shown in the figure 2.3.

The rate of formation of volatiles from pyrolysis is expressed as:

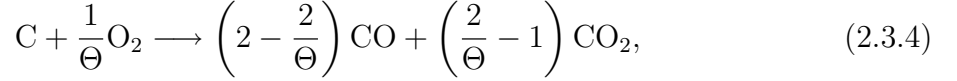
$$r_{vol} = k_{vol} m_{vol}, \quad k_{vol} = 1,56 \cdot 10^{10} \exp\left(-\frac{16\,600}{T_s}\right), \quad (2.3.3)$$

where  $k_{vol}$  is the rate constant of devolatilization, depending on the temperature of the solid fuel  $T_s$ , and  $m_{vol}$  is the mass of volatiles remaining in the fuel.

### 2.3.3 Char oxidation

Char forms as volatiles escape from the biomass particles. The primary products of char oxidation are CO and CO<sub>2</sub>. Under the assumption that char contains carbon only, the

char oxidation reaction is:



where

$$\Theta = \frac{1 + \frac{1}{r_c}}{0.5 + \frac{1}{r_c}} \quad (2.3.5)$$

is the stoichiometric ratio for char combustion,  $r_c$  is the ratio of  $\frac{\text{CO}}{\text{CO}_2}$  formation rates, which can be calculated using the following formula:

$$r_c = 12 \exp\left(-\frac{3300}{T_s}\right). \quad (2.3.6)$$

The rate of consumption of  $\text{O}_2$  during char oxidation follows from the chemical reaction (2.3.4) and it is given by

$$r_{\text{O}_2} = \frac{1}{\Theta} \frac{M_{\text{O}_2}}{M_C} r_{\text{char}}, \quad (2.3.7)$$

where  $M_{\text{O}_2}$  and  $M_C$  is molar mass of oxygen and carbon, respectively. Finally, the overall reaction rate of char oxidation is:

$$r_{\text{char}} = k_o m_{\text{char}} p_{\text{O}_2}, \quad (2.3.8)$$

where  $m_{\text{char}}$  is the mass of char remaining in the straw,  $p_{\text{O}_2}$  is partial pressure of  $\text{O}_2$  in the gas, and

$$k_o = \frac{\Theta W_{\text{char}} k_d k_c}{(r_{\text{ext}} - r_{\text{in}}) \rho_{\text{char}} R T_s k_c + \Theta W_{\text{char}} k_d} \quad (2.3.9)$$

is the overall reaction rate constant. Here,  $\rho_{\text{char}}$  is the char density in the straw wall,  $W_{\text{char}}$  is the molecular weight of carbon,  $R$  is the ideal gas constant, and

$$k_c = 8620 \exp\left(-\frac{15900}{T_s}\right) \quad (2.3.10)$$

is the rate constant of char oxidation. Since

$$r_{\text{char}} + r_{\text{O}_2} = r_{\text{CO}} + r_{\text{CO}_2} = r_c r_{\text{CO}_2} + r_{\text{CO}_2} = r_{\text{CO}_2} (1 + r_c), \quad (2.3.11)$$

the rate of  $\text{CO}_2$  production due to the char combustion is

$$r_{\text{CO}_2, c} = \frac{r_{\text{char}} + r_{\text{O}_2}}{1 + r_c}. \quad (2.3.12)$$

The corresponding rate of  $\text{CO}$  production from the char combustion  $r_{\text{CO}, c}$  is then calculated using (2.3.6).

It is now good to note that a huge amount of effort has been spent on finding good (mostly empirical) relations for coefficients such as  $k_v$ ,  $k_d$ ,  $k_c$ ,  $\Theta$  that would well represent all processes. These relations are derived using Arrhenius expression. Various authors (like [3], [6], [10]) propose different pre-exponential factors and activation energies which appear in Arrhenius expression, so the resulting rate constants are also different. As will be shown later, these coefficients play an important role during the tuning of the computational model. .

## 2.4 Governing equations

The overall combustion process is governed by a system of partial differential equations (PDE), two of which describe the mass and energy conservation laws for the solid phase, while the rest of the equations are the continuity equations for the gas and individual gas-phase species, and energy equation of the gas phase [6]. The governing equations are nonlinear, thus a suitable numerical method has to be implemented to find the solution of the system. The independent variables are time  $t \in \langle 0, \tau \rangle$ , and one space variable  $x \in \langle 0, h_b \rangle$ , where  $x = 0$  is set at the bottom of the bed, and  $h_b$  is the bed height. More detailed analysis of each equation is provided in the following.

### 2.4.1 Solid phase PDE's

#### 1. Mass conservation equation

$$\frac{\partial \rho_s}{\partial t} = -r_f \quad (2.4.13)$$

The equation describes the rate of change of the bulk density of straw bed. The source term  $r_f$  is the conversion rate from solid to gas due to moisture evaporation, devolatilization, and char oxidation. Therefore,

$$r_f = r_{H_2O} + r_{vol} + r_{char}. \quad (2.4.14)$$

The bulk density of straw bed is defined as

$$\rho_s = \frac{m_s}{V}, \quad m_s = m_{H_2O} + m_{vol} + m_{char} + m_{ash}, \quad (2.4.15)$$

where  $m_s$  is the mass of the solid fuel in the volume  $V$ ,  $V = V_f + V_s$ , where  $V_f$  and  $V_s$  are those parts of volume  $V$  occupied by the gas and the solid fuel, respectively. Since both  $V$  and  $m_{ash}$  are constant, equation (2.4.13) can be rewritten in the form

$$\frac{\partial m_s}{\partial t} = \frac{\partial m_{H_2O}}{\partial t} + \frac{\partial m_{vol}}{\partial t} + \frac{\partial m_{char}}{\partial t} = -r_f V. \quad (2.4.16)$$

Individual rates of mass changes are given by

$$\frac{\partial m_{H_2O}}{\partial t} = -r_{H_2O} V, \quad \frac{\partial m_{vol}}{\partial t} = -r_{vol} V, \quad \frac{\partial m_{char}}{\partial t} = -r_{char} V. \quad (2.4.17)$$

Equations (2.4.17) describe the rates of changes of individual mass components of the fuel. Hence solving these equations the bulk density  $\rho_s$  is solved as well.

#### 2. Energy equation

$$\frac{\partial (\rho_s h_s)}{\partial t} = \frac{\partial}{\partial x} \left( k_{eff} \frac{\partial T_s}{\partial x} \right) + hS(T_f - T_s) + Q_s + Q_{H_2O} + Q_r \quad (2.4.18)$$

The equation expresses the law of conservation of energy in the solid phase. Beside a number of coefficients and source terms, it introduces two thermodynamic state quantities - namely the specific enthalpy  $h_s$  and temperature  $T_s$ . Since

$$dh = c_p dT, \quad (2.4.19)$$

where  $c_p$  is specific heat capacity at constant pressure, holds for ideal gases and incompressible substances [11], the energy equation (2.4.18) can be rewritten into the form

$$\frac{\partial (\rho_s h_s)}{\partial t} = \frac{\partial}{\partial x} \left( \frac{k_{eff}}{c_{p,s}} \frac{\partial h_s}{\partial x} \right) + hS(T_f - T_s) + Q_s + Q_{H_2O} + Q_r. \quad (2.4.20)$$

Through the relation (2.4.19) one can choose whether to solve the energy equation with respect to  $h_s$  or  $T_s$ . According to [12], for a perfect polytropic gas,  $c_p$  is constant and the equation (2.4.19) becomes

$$h = c_p T, \quad (2.4.21)$$

and so rewriting of the equation (2.4.18) to be solved for the temperature is straightforward. However, gases are rarely described as perfect in practice. Instead, they are treated as ideal, so the state equations still hold, but physical quantities such as  $c_p$  are not constant [13]. This implies that the relation (2.4.19) must be integrated from a reference state to the final one. The next step is to use the mean integral value to obtain

$$\Delta h = h_{final} - h_{ref} = \int_{T_{ref}}^{T_{final}} c_p dT = \bar{c}_p \Delta T. \quad (2.4.22)$$

The specific heat capacity of the solid phase  $c_{p,s}$ , and its mean value  $\bar{c}_{p,s}$  are:

$$c_{p,s} = 977,75 \ln T_s - 4144,4 \quad [6], \quad \bar{c}_{p,s} = \frac{1}{\Delta T_s} \int_{T_{s,ref}}^{T_{s,final}} c_{p,s} dT_s. \quad (2.4.23)$$

The relation (2.4.22) can be used to obtain either temperature  $T_s$  on the right hand side of (2.4.20) or the enthalpy  $h_s$  in (2.4.18). If the enthalpy  $h_{ref}$  is defined to be zero at the temperature state  $T_{ref}$ , then

$$T_s = \frac{h_s}{\bar{c}_{p,s}} + T_{s,ref}, \quad h_s = \bar{c}_{p,s} \Delta T_s \quad (2.4.24)$$

The energy equation (2.4.18) can now be expressed in terms of temperature:

$$\frac{\partial (\rho_s \bar{c}_{p,s} (T_s - T_{s,ref}))}{\partial t} = \frac{\partial}{\partial x} \left( k_{eff} \frac{\partial T_s}{\partial x} \right) + hS(T_f - T_s) + Q_s + Q_{H_2O} + Q_r. \quad (2.4.25)$$

There are however other quantities in the energy equation of the solid phase, that have not been described yet. The  $h$  is the gas-solid heat transfer coefficient. The effective thermal conductivity  $k_{eff}$  is expressed as [6]:

$$k_{eff} = k_{eff,0} + \frac{0,5k_f Pr Re}{\epsilon_b}, \quad (2.4.26)$$

where  $k_{eff,0}$  is the thermal conductivity for no fluid flow,  $k_f$  is the thermal conductivity of the gas phase, and  $Pr$  is the Prandtl number. The  $k_{eff,0}$  is given [5] by

$$k_{eff,0} = 2,27 \cdot 10^{-6} \cdot T_s^{1,85}. \quad (2.4.27)$$

The Reynolds number  $Re$  is given by

$$Re = \frac{2\rho_f v_f r_{ext}}{\nu_f}, \quad (2.4.28)$$

where  $v_f$  is the gas velocity, and  $\nu_f$  is the gas viscosity depending on the gas temperature  $T_f$  [9]

$$\nu_f = 1,98 \cdot 10^{-5} \left( \frac{T_f}{300} \right)^{\frac{2}{3}}. \quad (2.4.29)$$

The porosity of the bed  $\epsilon_b$  is defined as

$$\epsilon_b = \frac{V_f}{V} = 1 - \frac{\rho_s}{\rho_{straw}}, \quad (2.4.30)$$

where  $\rho_{straw}$  is the density of the straw wall (i.e. material density of the fuel). The assumption of no volume reduction is important here. It means that the porosity  $\epsilon_b$  is constant. The source terms  $Q_{H_2O}$ ,  $Q_s$ ,  $Q_r$  represent the heat loss due to moisture evaporation, the heat gain due to the char combustion, and the radiative heat source, respectively. It is important to note that, in fact,  $Q_{H_2O} < 0$ .

## 2.4.2 Gas phase PDE's

### 1. Continuity equation

$$\frac{\partial(\epsilon_b \rho_f)}{\partial t} + \frac{\partial(\rho_f v_f)}{\partial x} = r_f \quad (2.4.31)$$

The equation describes the rate of change of mass of the gas phase. The source term  $r_f$  is defined by (2.4.14),  $\rho_f$  is the gas density, which can be expressed via thermodynamic state equation as

$$\rho_f = \frac{p}{r T_f}, \quad (2.4.32)$$

where  $p$  is the gas pressure,  $T_f$  is the gas temperature, and  $r$  is the specific gas constant. The continuity equation (2.4.31) is solved to obtain the gas velocity  $v_f$ .

Due to the assumption of plug-flow and knowledge of the rates of mass conversion, the velocity  $v_f$  can also be calculated via the mass flow rate. In a steady one-dimensional flow, the mass flow rate through an arbitrary cross-sectional area is constant [13]. The problem given here is unsteady, so it is not constant, but still must be conserved. If  $\dot{m}_{S_1}$  is the mass flow rate through the cross-sectional area  $S_1$  and  $\dot{m}_{S_2}$  the mass flow rate through the cross-sectional area  $S_2$  that is placed in the upstream direction from  $S_1$ , then the difference  $\dot{m}_{S_2} - \dot{m}_{S_1}$  is equal to the mass flow rate from the solid phase to the gas phase caused by the moisture evaporation, devolatilization, and the char combustion occurring in the volume in between the cross-sectional areas  $S_1$  and  $S_2$ . Thus,

$$\dot{m}_{S_2} = \dot{m}_{S_1} + r_f V_{S_1 S_2}. \quad (2.4.33)$$

If the cross-sectional areas are perpendicular to the flow direction, the velocity  $v_{f,S}$  at  $x = x_S$  can be obtained by

$$v_{f,S} = \frac{\dot{m}_S}{\rho_f S \epsilon_b}. \quad (2.4.34)$$



It is clear that under these conditions the equation (2.4.31) needs not to be solved. Instead, one can choose to obtain the velocity field via (2.4.34).

## 2. Gas species continuity equation

$$\frac{\partial (\epsilon_b \rho_f X_i)}{\partial t} + \frac{\partial (\rho_f v_f X_i)}{\partial x} = \frac{\partial}{\partial x} \left( \epsilon_b \rho_f D_{a,eff} \frac{\partial X_i}{\partial x} \right) + \epsilon_b r_i \quad (2.4.35)$$

This PDE describes the mass transfer of individual gas species subscripted by  $i$ ,  $i \in \{\text{CO}, \text{CO}_2, \text{O}_2, \text{N}_2, \text{C}_2\text{H}_6, \text{H}_2\text{O}, \text{H}_2\}$ . The source term  $r_i$  represents the rate of mass production of the gas species during moisture evaporation, devolatilization, and the char combustion,  $D_{a,eff}$  is a so-called effective axial dispersion coefficient [6]:

$$D_{a,eff} = D_i + 0.5 v_f d_{ext}, \quad (2.4.36)$$

where  $d_{ext} = 2r_{ext}$  is the external diameter of straw, and  $D_i$  is the molecular diffusion coefficient [14]. Due to data unavailability, the coefficients  $D_{C_2H_6}$  and  $D_{H_2}$  are taken as  $D_{CH_4}$  and  $D_{N_2}$ , respectively. The species continuity equation is solved with respect to the mass fraction of the species  $X_i$ . The specific gas constant  $r$  used in (2.4.32) is a function of the unknowns  $X_i$ :

$$r = R \sum_i \frac{X_i}{M_i}. \quad (2.4.37)$$

Here,  $R$  is the ideal gas constant, and  $M_i$  is the molar mass of the species.

## 3. Energy equation

$$\frac{\partial (\epsilon_b \rho_f h_f)}{\partial t} + \frac{\partial (\rho_f v_f h_f)}{\partial x} = \frac{\partial}{\partial x} \left( \epsilon_b k_f \frac{\partial T_f}{\partial x} \right) + hS(T_s - T_f) \quad (2.4.38)$$

This equation is similar to the one of the solid phase. Furthermore, the result in (2.4.24) is applicable again (with corresponding subscripts for the gas phase - fluid), and one can make a choice to solve the equation either for the specific enthalpy  $h_f$  (2.4.39) or temperature  $T_f$  (2.4.40):

$$\frac{\partial (\epsilon_b \rho_f h_f)}{\partial t} + \frac{\partial (\rho_f v_f h_f)}{\partial x} = \frac{\partial}{\partial x} \left( \epsilon_b \frac{k_f}{c_{p,f}} \frac{\partial h_f}{\partial x} \right) + hS(T_s - T_f) \quad (2.4.39)$$

$$\frac{\partial (\epsilon_b \rho_f \bar{c}_{p,f} (T_f - T_{f,ref}))}{\partial t} + \frac{\partial (\rho_f v_f \bar{c}_{p,f} (T_f - T_{f,ref}))}{\partial x} = \frac{\partial}{\partial x} \left( \epsilon_b k_f \frac{\partial T_f}{\partial x} \right) + hS(T_s - T_f) \quad (2.4.40)$$

The specific heat capacity  $c_{p,f}$  and its mean value  $\bar{c}_{p,f}$  are given by:

$$c_{p,f} = (0.99 + 1.22 \cdot 10^{-4} T_f - 5.68 \cdot 10^{-3} T_f^{-2}) \cdot 10^3 \quad [6], \quad (2.4.41)$$

$$\bar{c}_{p,f} = \frac{1}{\Delta T_f} \int_{T_{f,ref}}^{T_{f,final}} c_{p,f} dT_f. \quad (2.4.42)$$

The thermal conductivity  $k_f$  in (2.4.38) can be obtained [6] by:

$$k_f = 4,8 \cdot 10^{-4} T_f^{0,717}. \quad (2.4.43)$$

Now it is important to say a word about the gas thermal conductivity (2.4.43) as well as the specific heat capacities (2.4.23) and (2.4.41) which all have been cited from [6]. The author introduces (2.4.43) with different exponent, namely with  $10^4$ . Such an exponent makes the coefficient (2.4.43) extremely large. At least, one would expect the order of value of  $k_f$  to be comparable with orders of some common gases that can be found for instance in [15]. Zhou [6] also introduces similar temperature relation for the air thermal conductivity with the exponent  $10^{-5}$ . This leads to the conclusion that the relation for  $k_f$  was originally intended to be written as (2.4.43).

A similar situation arises with the heat capacities which are expressed in  $[\text{J mol}^{-1}\text{K}^{-1}]$  units, while other quantities in the energy equations have physical dimension of  $[\text{kg m}^{-3}]$ . Therefore either capacity or all corresponding quantities must be recalculated by use of molar masses. These again results in much larger values for the heat capacity (the same reference can be used for comparison) than it would be expected from a gas at ambient conditions. Without any recalculation the relation (2.4.41) gives expected values, so it is probably already expressed in desirable units. Although values of the heat capacity of straw (2.4.23) have not been compared with another reference, the relation (2.4.23) is assumed to be expressed in  $[\text{J kg}^{-1}\text{K}^{-1}]$  units.

## 2.5 Initial and boundary conditions

To complete the system of PDE's it is necessary to formulate initial and boundary conditions, which determine a unique solution. While the initial conditions do not give much trouble, stating the boundary conditions is sometimes problematic. Even for a simple linear ordinary differential equation with boundary conditions it can happen that the solution to the equation does not exist or there are infinitely many of them [16]. Because of the physical nature of the given problem, such a situation however cannot arise, therefore boundary conditions should reflect the system's behaviour to give a unique solution. For both types of conditions, conditions for specific enthalpies are not explicitly written, since they can be calculated from given temperatures using (2.4.22).

### 2.5.1 Initial conditions

These conditions describe the states of the solid and gas phases at the beginning of the process, i.e. for  $t = 0$ . Usually, they correspond with the ambient conditions.

For  $\forall x \in \langle 0, h_b \rangle = \langle A, B \rangle$

$$\begin{aligned} \text{solid phase: } m_s(x, 0) &= m_{s,0}, & T_s(x, 0) &= T_{s,0} \\ \text{gas phase: } v_f(x, 0) &= v_{f,0}, & X_i(x, 0) &= X_{i,0}, & T_f(x, 0) &= T_{f,0} \end{aligned} \quad (2.5.44)$$

## 2.5.2 Boundary conditions

At the bottom of the bed the Dirichlet conditions for the mass flow rate (or velocity), gas temperature and the mass fractions of gas species are given by operating conditions, while for the solid temperature Neumann boundary condition is applied and its value is assumed to be zero. At the top surface of the bed, gradients of all unknown functions are also set to zero.

For  $\forall t \in \langle 0, \tau \rangle$

$$\begin{aligned}
 \text{solid phase: } \quad & \frac{\partial T_s(A,t)}{\partial x} = 0, & \frac{\partial T_s(B,t)}{\partial x} = 0 \\
 \text{gas phase: } \quad & v_f(A,t) = v_{f,A}, & \frac{\partial v_f(B,t)}{\partial x} = 0 \\
 & X_i(A,t) = X_{i,A}, & \frac{\partial X_i(B,t)}{\partial x} = 0 \\
 & T_f(A,t) = T_{f,A} & \frac{\partial T_f(B,t)}{\partial x} = 0
 \end{aligned} \tag{2.5.45}$$

As it has been mentioned the boundary conditions must be reflecting the real behaviour of the system on the boundaries of the computational domain. The energy equation (2.4.20) takes into account the radiation heat source  $Q_r$  which is usually placed on the top of the bed. However, this would not coincide with the zero-gradient Neumann boundary conditions at  $x = B$ , since obviously there would be a nonzero heat influx. Some authors like Zhou [6], Yang [10], formulate the boundary condition via the ignition temperature as the over-bed radiation source (i.e. Dirichlet b.c. for solid). The approach used in the thesis is that the heat source is placed somewhere inside the bed, so zero gradients at the outflow can be used. If it was placed on the top of the bed, it would influence gradients of other quantities, too.

## 2.6 Summary

The mathematical model formed by governing and process rate equations, and completed by initial and boundary conditions has been presented. The system of PDE's is nonlinear, so the solution must be found by a numerical method. The selection of the method as well as numerical formulation of the problem and implementation with interpretation of results are the objectives of the next chapter.

# Chapter 3

## Numerical model

The previous chapter has described the mathematical model of the grate combustion processes occurring in a furnace with a fixed bed. These processes are governed by a system of several PDE's that, together with process rate equations, form quite a complex system of equations. Due to the complexity the solution cannot be obtained by an analytical method.

### 3.1 Selection of the method

Numerical mathematics plays an important role in the field of engineering calculations and provides a number of ways for finding the solution of complex problems. Generally, there are three basic groups of numerical methods for solving PDE's - the finite difference method (FDM), the finite volume method (FVM) and the finite element method (FEM). The FDM is the oldest one among them, but is still being utilized in problems defined in domains like a line segment, square, rectangle etc. While the FEM is mostly used in mechanics of solids, the FVM has endeared on solving problems concerning the prediction of fluid flow. It is caused mainly by the simplicity of the method and its simple and straightforward compliance with the conservation laws even for the most complex equations, that is of the biggest importance [12], [16]. This is the key reason to choose the FVM for discretizing fluid flow governing equations. Moreover, for purposes of the future generalization and extension of the model up to three dimensions where the use of the FDM is very limited, this also gives the priority to use the FVM.

### 3.2 Discretization

There are many books written on the topic of fluid dynamics. A comprehensive description of discretization techniques and numerous finite volume schemes with stability and convergence analysis can be found in [17], [18]. Also the book written by Patankar [19] has become very popular among CFD users. The discretization of the governing equations in the present work is based mostly on this book.

Since the unknowns are functions of the time variable  $t$  and spatial variable  $x$ , the discretization must be carried out for both of these dimensions.

### 3.2.1 General transport equation

Mass, momentum and heat transfer is generally described by a system of PDE's, which includes the continuity equation, the Navier-Stokes equations of motion of viscous fluids (in case of inviscid fluids, we have the Euler equations), and the energy equation. All dependent variables appearing in the system seem to obey a generalized conservation principle [19]. The governing equations can be expressed by a single PDE called general transport equation. Its one-dimensional form is given by:

$$\frac{\partial(\rho\phi)}{\partial t} + \frac{\partial(\rho u\phi)}{\partial x} = \frac{\partial}{\partial x} \left( \Gamma \frac{\partial\phi}{\partial x} \right) + S_\phi. \quad (3.2.1)$$

Of course, the unknown  $\phi$ , the diffusion coefficient  $\Gamma$  as well as the source term  $S_\phi$  must be given appropriate meanings with respect to the equation represented by (3.2.1). Therefore there is no need to discretize all governing PDE's alone. Instead, the discretization concept will be shown on (3.2.1) and the result will be directly applied to particular equations described before.

### 3.2.2 Spatial discretization

The FVM is based on dividing the computational domain into a finite number of nonoverlapping subdomains called control volumes or cells<sup>1</sup>, and integrating PDE's over each cell. First, the so called basic mesh is defined by a set of points (nodes) from the domain, and then a dual mesh is constructed upon the basic mesh, so that to each node a control volume is assigned.

The computational domain in this work is a line segment  $\Omega = \langle A, B \rangle$  (note that  $A = 0$  and  $B = h_b$  as mentioned before in the section with initial and boundary conditions). Let  $x_i = (i - \frac{1}{2})\Delta x$ ,  $i = 1, \dots, N$  be a set of equidistant nodes, where  $\Delta x = B/N$ . To simplify the notation, letters  $W, P, E$  will denote the nodes  $x_{i-1}, x_i, x_{i+1}$ , respectively, according to the standard notation widely used in books on the subject (also in [19]). The interval  $\langle A, B \rangle$  is uniformly divided into  $N$  subintervals, each of which is assigned to a node. So,  $\Omega = \cup_{i=1}^N \langle x_{i-1/2}, x_{i+1/2} \rangle$ , where  $x_{i-1/2} = x_i - \frac{1}{2}\Delta x$ ,  $x_{1/2} = A$ ,  $x_{N+1/2} = B$ . Also here a simplified notation will be used, so that the points  $x_{i-1/2}, x_{i+1/2}$  at the cell faces will be denoted by letters  $e, w$ , respectively<sup>2</sup>. The situation is shown in the figure 3.1. The goal is to evaluate an unknown function at the nodes  $P$ .

The equation (3.2.1) is integrated over each control volume. This yields:

$$\int_w^e \frac{\partial(\rho\phi)}{\partial t} dx + (\rho u\phi)_e - (\rho u\phi)_w = \left( \Gamma \frac{\partial\phi}{\partial x} \right)_e - \left( \Gamma \frac{\partial\phi}{\partial x} \right)_w + \bar{S}\Delta x, \quad (3.2.2)$$

where  $\bar{S}$  is the average value of  $S_\phi$  over the control volume. The subscript  $\phi$  has been omitted for simplicity of notation. Since each PDE is going to become a system of discretized equations that are solved by the techniques of linear algebraic equations, the source term which often depends on the unknown  $\phi$  must be linearized into the form

$$\bar{S} = S_C - S_P\phi_P, \quad (3.2.3)$$

---

<sup>1</sup>Proper mathematical definitions of the discretization technique can be found in [12]. Here, the term nonoverlapping subdomains means that the intersection of any two control volumes is either an empty set, or common boundary of the two cells, or exactly one common point.

<sup>2</sup>The letters  $E, W$  stand for the eastern and western neighbours of the point  $P$ , respectively; the letters  $e, w$  are the eastern and western cell faces, respectively.

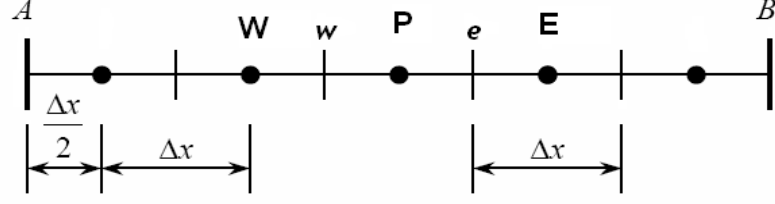


Figure 3.1: Discretization of the computational domain

where  $S_C$  is the constant part of  $\bar{S}$ , and  $S_P$  is the coefficient of  $\phi_P$ . The relation (3.2.3) should represent the true dependence of  $\bar{S}$  on  $\phi$  as well as possible. A good way to approximate such dependence is to expand  $\bar{S}$  into the Taylor series of the first order. However, if  $\bar{S}$  is a complicated function of  $\phi$ , the expansion could be very time-consuming. In such cases it is always possible to linearize the whole  $\bar{S}$  as  $S_C$ . Using the central-difference scheme for derivatives in the diffusion term,

$$\left(\Gamma \frac{\partial \phi}{\partial x}\right)_e - \left(\Gamma \frac{\partial \phi}{\partial x}\right)_w = \frac{\Gamma_e}{\Delta x} (\phi_E - \phi_P) - \frac{\Gamma_w}{\Delta x} (\phi_P - \phi_W), \quad (3.2.4)$$

where  $\Gamma_e, \Gamma_w$  is the value of the diffusion coefficient  $\Gamma$  at the eastern and western cell face, respectively. The simplest way to calculate these values is linear interpolation of values of the neighbouring nodes, i.e.

$$\Gamma_e = \frac{\Gamma_P + \Gamma_E}{2}, \quad \Gamma_w = \frac{\Gamma_P + \Gamma_W}{2}. \quad (3.2.5)$$

To simplify the notation, let  $D = \Gamma/\Delta x$ . Then the right side of the equation (3.2.4) becomes

$$\frac{\Gamma_e}{\Delta x} (\phi_E - \phi_P) - \frac{\Gamma_w}{\Delta x} (\phi_P - \phi_W) = D_e(\phi_E - \phi_P) - D_w(\phi_P - \phi_W). \quad (3.2.6)$$

Since central differencing used for discretization of the convective term suffers from boundedness for values of the Peclet number  $Pe > 2$ , and has no transportiveness (it does not propagate information about the flow in the flow direction), it is not suitable for further use [1]. Instead, the first order upwind scheme has been selected for discretization of the convective term. For simplicity of notation, let  $F = \rho u$ .

$$(F\phi)_e - (F\phi)_w = \max(F_e, 0) \phi_P - \max(-F_e, 0) \phi_E - \max(F_w, 0) \phi_W + \max(-F_w, 0) \phi_P, \quad (3.2.7)$$

where  $F_e, F_w$  are to be obtained by linear interpolation again as in (3.2.5). Since

$$a = \max(a, 0) - \max(-a, 0) \quad (3.2.8)$$

holds for any quantity  $a$ , the equation (3.2.7) can be rewritten into the form

$$\begin{aligned} (F\phi)_e - (F\phi)_w = & \left( \max(F_w, 0) + \max(-F_e, 0) + F_e - F_w \right) \phi_P - \\ & - \max(F_w, 0) \phi_W - \max(-F_e, 0) \phi_E. \end{aligned} \quad (3.2.9)$$

The time term from (3.2.2) is discretized in space using a constant profile over the cell as follows:

$$\int_w^e \frac{\partial(\rho\phi)}{\partial t} dx = \frac{\partial(\rho_P\phi_P)}{\partial t} \Delta x. \quad (3.2.10)$$

For further use it is worth to rearrange all discretized terms in this way:

$$\begin{aligned} \frac{\partial(\rho_P\phi_P)}{\partial t} \Delta x + \left( \max(F_w, 0) + \max(-F_e, 0) + F_e - F_w + D_e + D_w + S_P \Delta x \right) \phi_P = \\ = \left( \max(-F_e, 0) + D_e \right) \phi_E + \left( \max(F_w, 0) + D_w \right) \phi_W + S_C \Delta x. \end{aligned} \quad (3.2.11)$$

### 3.2.3 Temporal discretization

The time interval  $(0, \tau)$  has been divided into  $M$  subintervals of the same length, so the time step  $\Delta t = \tau/M$ . Temporal discretization has been carried out by the implicit Euler method. The advantage of the method is its unconditional stability with respect to the chosen time step. On the other hand, this also brings a problem to solve a system of algebraic equations in contrast to the explicit Euler method, which requires nothing but a simple enumeration. The equation (3.2.11) is integrated over a time step and then divided by  $\Delta t$ :

$$\begin{aligned} \frac{\Delta x}{\Delta t} (\rho_P\phi_P - \rho_P^0\phi_P^0) + \left( \max(F_w, 0) + \max(-F_e, 0) + F_e - F_w + D_e + D_w + S_P \Delta x \right) \phi_P = \\ = \left( \max(-F_e, 0) + D_e \right) \phi_E + \left( \max(F_w, 0) + D_w \right) \phi_W + S_C \Delta x, \end{aligned} \quad (3.2.12)$$

where the superscript 0 denotes the known value of the quantity at the previous time  $t$ , while the values of quantities without the superscript are evaluated at the new time  $t + \Delta t$ , thus they are unknown. Again, to simplify the notation,

$$a_E = \left( \max(-F_e, 0) + D_e \right), \quad a_W = \left( \max(F_w, 0) + D_w \right), \quad (3.2.13)$$

and so (3.2.12) turns into

$$\left( a_E + a_W + F_e - F_w + S_P \Delta x + \frac{\Delta x}{\Delta t} \rho_P \right) \phi_P = a_E \phi_E + a_W \phi_W + a_P^0 \phi_P^0 + S_C \Delta x, \quad (3.2.14)$$

where  $a_P^0 = \frac{\Delta x}{\Delta t} \rho_P^0$ .

### 3.2.4 Final discretization equation

It is important to say that while solving the discretization equation (3.2.14), the flow field must satisfy the continuity equation

$$\frac{\partial \rho}{\partial t} + \frac{\partial(\rho u)}{\partial x} = \tilde{R}, \quad (3.2.15)$$

where  $\tilde{R}$  is the source term such as  $r_f$  from (2.4.14). Fluent [2] uses two types of solvers, namely the pressure-based solver and the density-based solver. The first one is based on

the SIMPLE algorithm [19], in which the velocity field is calculated from the momentum equations and corrected by the pressure correction obtained from the continuity equation. Afterwards, the other scalar quantities like enthalpy, chemical species, etc. are obtained. Such a procedure is inapplicable here, since no momentum equation is given and the pressure is assumed to be constant. To obtain the scalar quantity  $\phi$  while satisfying the continuity equation, the equation (3.2.15) is discretized:

$$\frac{\Delta x}{\Delta t}(\rho_P - \rho_P^0) + F_e - F_w = \tilde{R}_C \Delta x, \quad (3.2.16)$$

where  $\tilde{R}_C$  is the linearization of  $\tilde{R}$  by a constant. Subtracting  $\tilde{R}_C \Delta x$  from the equation (3.2.16) and multiplying the equation by  $\phi_P$  leads to

$$\left( \frac{\Delta x}{\Delta t} \rho_P - \frac{\Delta x}{\Delta t} \rho_P^0 + F_e - F_w - \tilde{R}_C \Delta x \right) \phi_P = 0, \quad (3.2.17)$$

and subtracting (3.2.17) from (3.2.14) gives

$$\left( a_E + a_W + a_P^0 + S_P \Delta x + \tilde{R}_C \Delta x \right) \phi_P = a_E \phi_E + a_W \phi_W + a_P^0 \phi_P^0 + S_C \Delta x. \quad (3.2.18)$$

Indeed, the last few steps made for derivation of the final discretization equation have a physical interpretation. When the flow field is correct (i.e. it satisfies (3.2.15)), the solution obtained from (3.2.14) is also correct and satisfies the multiplied continuity equation (3.2.17). Since this equation is a part of (3.2.14), (3.2.18) and (3.2.14) both yield the same solution. On the other hand, if the continuity equation is not satisfied, these two equations lead to different solutions. Preferable solution is the one obtained from (3.2.18), since it takes into account the continuity equation.

Before writing the final form of the general discretization equation, a simplification of coefficients  $a_E, a_W$  can be made. The assumption of plug-flow determines the flow direction, so  $\max(-F_e, 0) = 0$ , and  $\max(F_w, 0) = F_w$ .

The final form of the general discretization equation is given by

$$a_P \phi_P = a_E \phi_E + a_W \phi_W + a_P^0 \phi_P^0 + S_C \Delta x \quad (3.2.19)$$

$$a_E = D_e \quad (3.2.20)$$

$$a_W = F_w + D_w \quad (3.2.21)$$

$$a_P^0 = \frac{\Delta x}{\Delta t} \rho_P^0 \quad (3.2.22)$$

$$a_P = a_E + a_W + a_P^0 + (S_P + \tilde{R}_C) \Delta x \quad (3.2.23)$$

The equation (3.2.19) represents a sparse tridiagonal system of  $N$  algebraic equations. Such a system is better solved iteratively rather than by a direct method, since the iterative procedure utilizes the sparsity of the system, and so uses less computer memory. It follows that the system matrix should have the properties that guarantee the convergence of an iterative process. For the point-by-point Gauss-Seidel method, the matrix should be diagonally dominant [20], i.e.

$$|a_P| > \sum |a_{nb}|, \text{ for } \forall P, \quad \text{where } nb \text{ denotes the neighbouring points.} \quad (3.2.24)$$



It is sufficient to satisfy the so called Scarborough criterion, in which the strict inequality (3.2.24) is required only for one point at least [19]. If  $\tilde{R}_C \geq 0$ , then the given inequality is always satisfied. If  $\tilde{R}_C < 0$ , then the coefficient  $a_P$  might become smaller than the sum of other neighbouring coefficients, or even negative. To avoid this, if  $\tilde{R}_C < 0$ , then it is removed from  $a_P$ ,  $\tilde{R}_C \phi_P \Delta x$  is linearized by a constant, and added to the right hand side of (3.2.19). However, if the absolute value  $|\tilde{R}_C|$  is small compared to the value of  $S_P$ , there is no need to do such modifications, since the diagonal dominance (or the Scarborough criterion) is satisfied.

### 3.2.5 Boundary conditions

The system of algebraic equations (3.2.19) is completed by applying the boundary conditions. Two cases are considered:

$$\begin{aligned} \text{Dirichlet b.c.: } \phi(A, t) = \phi_A \quad & \text{Neumann b.c.: } \frac{\partial \phi(A, t)}{\partial x} = 0 \\ & \frac{\partial \phi(B, t)}{\partial x} = 0 \end{aligned} \quad (3.2.25)$$

The boundary conditions determine the values at the cell faces on the boundaries of the computational domain. Therefore they appear in the coefficients  $D_e$ ,  $D_w$ ,  $F_e$ ,  $F_w$  defined only for the first and the last control volumes. The corresponding equations in the system (3.2.19) are given by:

- Dirichlet boundary condition  
 $x = A$ :

$$a_P \phi_P = a_E \phi_E + a_A \phi_A + a_P^0 \phi_P^0 + S_C \Delta x \quad (3.2.26)$$

$$a_E = D_e \quad (3.2.27)$$

$$a_A = F_A + 2D_A \quad (3.2.28)$$

$$a_P^0 = \frac{\Delta x}{\Delta t} \rho_P^0 \quad (3.2.29)$$

$$a_P = a_E + a_A + a_P^0 + (S_P + \tilde{R}_C) \Delta x \quad (3.2.30)$$

- Neumann boundary conditions  
 $x = A$ :

$$a_P \phi_P = a_E \phi_E + a_P^0 \phi_P^0 + S_C \Delta x \quad (3.2.31)$$

$$a_E = D_e \quad (3.2.32)$$

$$a_P^0 = \frac{\Delta x}{\Delta t} \rho_P^0 \quad (3.2.33)$$

$$a_P = a_E + a_P^0 + (S_P + \tilde{R}_C) \Delta x \quad (3.2.34)$$

$x = B$ :

$$a_P \phi_P = a_W \phi_W + a_P^0 \phi_P^0 + S_C \Delta x \quad (3.2.35)$$

$$a_W = F_w + D_w \quad (3.2.36)$$

$$a_P^0 = \frac{\Delta x}{\Delta t} \rho_P^0 \quad (3.2.37)$$

$$a_P = a_W + a_P^0 + (S_P + \tilde{R}_C) \Delta x \quad (3.2.38)$$

### 3.3 Iterative procedure

The system of PDE's is nonlinear. Thus, during each time step of the numerical solution, several iterations must be carried out until convergence is reached. Mathematics provides numerous approaches for solving nonlinear equations (or systems of equations). One of the basic methods recommended for solving a nonlinear system of equations obtained from the discretization of differential equations by an implicit method is the Newton method. However, Patankar [19] describes an iterative procedure that corresponds rather with the simple fixed-point iterative method. Such method is also used here. The coefficients of matrix of the system as well as the source terms are recalculated in each iteration from the values obtained in the previous iteration. The advantage is its simple implementation.

The criterion of convergence of the method is usually hard to verify in practice due to the complexity of all relations incident in the problem. Therefore, a control of how the discretization equations are satisfied by the current solution is a good way of measuring the convergence, too. This approach does not suffer from heavy underrelaxation which might cause an illusion of convergence, when examined just by the relative change of two successive solutions. The only exception is made for equations (2.4.17) where the implementation of the Newton method is quite simple due to the nature of these equations.

### 3.4 Application to the system of PDE's

Results from the previous sections is now applied to the governing equations described in the chapter 2.

#### 3.4.1 Solid phase

##### 1. Mass transfer equation

The conversion of mass of the solids is governed by (2.4.17). Due to the simplicity of the equations, it is possible to write discretized equations directly without any formulas derived in the previous sections.

$$\begin{aligned} m_{H_2O,P} &= m_{H_2O,P}^0 - r_{H_2O,P} V \Delta t \\ m_{vol,P} &= m_{vol,P}^0 - r_{vol,P} V \Delta t \\ m_{char,P} &= m_{char,P}^0 - r_{char,P} V \Delta t \end{aligned} \quad (3.4.39)$$

The equation for  $m_{vol}$  will be treated first. The rate of volatile release is a linear function of  $m_{vol}$  according to (2.3.3), so the new value of volatile mass can be

obtained without the use of an iterative method by

$$m_{vol,P} = \frac{m_{vol,P}^0}{1 + k_{vol,P} V \Delta t}. \quad (3.4.40)$$

For the rest of equations (3.4.39) the Newton method is implemented. The general scheme of the method for finding the roots of a function  $f(x)$  is given in [20] by

$$x^{k+1} = x^k - \frac{f(x^k)}{f'(x^k)}, \quad (3.4.41)$$

where  $k$  denotes the iteration. The function  $f(x)$  for equations (3.4.39) is given by

$$f(x) \equiv f(m_{i,P}) = m_{i,P} - m_{i,P}^0 + r_{i,P} V \Delta t, \quad (3.4.42)$$

where subscript  $i$  stands for  $H_2O, vol, char$ . The derivative of  $f(m_{i,P})$  with respect to  $m_{i,P}$  is

$$f'(m_{i,P}) = 1 + r'_{i,P} V \Delta t. \quad (3.4.43)$$

These derivatives are evaluated numerically by the first order forward difference scheme. Considering  $r_{i,P}$  to be a function of  $m_{i,P}$ , the scheme reads

$$f'(m_{i,P}) \approx 1 + \frac{r_{i,P}(m_{i,P} + \delta_{i,P}) - r_{i,P}(m_{i,P})}{\delta_{i,P}} V \Delta t, \quad (3.4.44)$$

where  $\delta_{i,P}$  is a sufficiently small step (change of mass  $m_{i,P}$ ).

## 2. Energy equation

A discretized form of the equation (2.4.20) will be shown. To simplify the notation, subscripts  $P$  will be omitted in all source terms. First of all, the term  $\tilde{R}_C = -r_f$  comes from the equation (2.4.13). Also, the source term  $\bar{S} = hS(T_f - T_s) + Q_{H_2O} + Q_s + Q_r$  is linearized to

$$\bar{S} = \underbrace{hS(T_f - T_{s,ref}) + Q_{H_2O} + Q_s + Q_r}_{S_C} - \underbrace{\frac{hS}{\bar{c}_s}}_{S_P} h_s, \quad (3.4.45)$$

and comparing the orders of expected values of terms  $S_P$  with  $\tilde{R}_C$ ,  $\tilde{R}_C h_{s,P} \Delta x$  should be treated as a constant and thus assigned to the right hand side of (3.2.19). The overall discretization equation is:

$$a_P h_{s,P} = a_E h_{s,E} + a_W h_{s,W} + a_P^0 h_{s,P}^0 + (S_C - \tilde{R}_C h_{s,P}^*) \Delta x, \quad (3.4.46)$$

where  $h_{s,P}^*$  is the value of the specific enthalpy from the previous iteration, and

$$a_E = \left( \frac{k_{eff}}{c_{p,s} \Delta x} \right)_e, \quad a_W = \left( \frac{k_{eff}}{c_{p,s} \Delta x} \right)_w, \quad a_P^0 = \frac{\Delta x}{\Delta t} \rho_{s,P}^0 \quad (3.4.47)$$

$$S_C = hS(T_f - T_{s,ref}) + Q_{H_2O} + Q_s + Q_r, \quad \tilde{R}_C = -r_f, \quad S_P = \frac{hS}{\bar{c}_{p,s}} \quad (3.4.48)$$

$$a_P = a_E + a_W + a_P^0 + S_P \Delta x \quad (3.4.49)$$

Boundary conditions: (only those equations that differ from (3.4.46)-(3.4.49))

$x = A :$

$$\begin{aligned} a_P h_{s,P} &= a_E h_{s,E} + a_P^0 h_{s,P}^0 + (S_C - \tilde{R}_C h_{s,P}^*) \Delta x \\ a_W &= 0 \\ a_P &= a_E + a_P^0 + S_P \Delta x \end{aligned} \quad (3.4.50)$$

$x = B :$

$$\begin{aligned} a_P h_{s,P} &= a_W h_{s,W} + a_P^0 h_{s,P}^0 + (S_C - \tilde{R}_C h_{s,P}^*) \Delta x \\ a_E &= 0 \\ a_P &= a_W + a_P^0 + S_P \Delta x \end{aligned} \quad (3.4.51)$$

### 3.4.2 Gas phase

Gas velocities are calculated from (2.4.34), so only the gas species and energy equations will be discretized.

#### 1. Gas species equation

All gas species equations will be discretized as one equation for  $X_i$ . There is no need to solve (2.4.35) for  $X_{N_2}$ , since  $\sum_i X_i = 1$ . The rates of production or consumption of individual gas species are expressed for each species. The overall discretization equation is:

$$a_P X_{i,P} = a_E X_{i,E} + a_W X_{i,W} + a_P^0 X_{i,P}^0 + S_C \Delta x, \quad (3.4.52)$$

$$a_E = \left( \frac{\epsilon_b \rho_f D_{a,eff}}{\Delta x} \right)_e, \quad a_W = (\rho_f v_f)_w + \left( \frac{\epsilon_b \rho_f D_{a,eff}}{\Delta x} \right)_w, \quad a_P^0 = \frac{\Delta x}{\Delta t} \epsilon_b \rho_{f,P}^0 \quad (3.4.53)$$

$$S_C = \epsilon_b r_i, \quad \tilde{R}_C = r_f, \quad S_P = 0 \quad (3.4.54)$$

$$a_P = a_E + a_W + a_P^0 + (S_P + \tilde{R}_C) \Delta x \quad (3.4.55)$$

The rates of production of  $H_2$ ,  $C_2H_6$ ,  $CO$ ,  $CO_2$  from the devolatilization and char combustion processes are defined in the sections 2.3.2 and 2.3.3. Total rates of production of different species  $r_i$  follow.

$$\begin{aligned} r_{CO} &= \gamma_1 r_{vol} + r_{CO,c}, & r_{C_2H_6} &= \gamma_3 r_{vol} \\ r_{CO_2} &= \gamma_2 r_{vol} + r_{CO_2,c}, & r_{H_2} &= \gamma_4 r_{vol} \end{aligned} \quad (3.4.56)$$

The rate of  $O_2$  consumption is given by (2.3.7), but it has a negative value in the equation (2.4.35), since it describes the consumption of  $O_2$ . Finally,  $r_{H_2O}$  is given by (2.3.1). It is important to note here that  $r_{H_2O}$  is a linear function of  $X_{H_2O}$  and so it should be linearized according to (3.2.3). It results in nonzero  $S_P$  and modified  $S_C$  as shown in (3.4.57). Concentrations  $C_{w,s}$  and  $C_{w,f}$  are defined as mass of water matter

per volume of the solid phase and gas phase, respectively. Then the linearization is given by:

$$\epsilon_b r_{H_2O} = \epsilon_b k_d S C_{w,s} - \epsilon_b k_d S C_{w,f} = S_C - \underbrace{\epsilon_b k_d S \rho_f}_{S_P} X_{H_2O} \quad (3.4.57)$$

Boundary conditions:

$x = A$  :

$$\begin{aligned} a_P X_{i,P} &= a_E X_{i,E} + a_A X_{i,A} + a_P^0 X_{i,P}^0 + S_C \Delta x \\ a_A &= (\rho_f v_f)_A + 2 \left( \frac{\epsilon_b \rho_f D_{a,eff}}{\Delta x} \right)_A \\ a_P &= a_E + a_A + a_P^0 + (S_P + \tilde{R}_C) \Delta x \end{aligned} \quad (3.4.58)$$

$x = B$  :

$$\begin{aligned} a_P X_{i,P} &= a_W X_{i,W} + a_P^0 X_{i,P}^0 + S_C \Delta x \\ a_E &= 0 \\ a_P &= a_W + a_P^0 + (S_P + \tilde{R}_C) \Delta x \end{aligned} \quad (3.4.59)$$

## 2. Energy equation

Treatment of the equation is similar to that one of the solid phase. The difference is in the source term  $\tilde{R}_C$  which is now positive. The overall discretization equation is:

$$a_P h_{f,P} = a_E h_{f,E} + a_W h_{f,W} + a_P^0 h_{f,P}^0 + S_C \Delta x, \quad (3.4.60)$$

$$a_E = \left( \frac{\epsilon_b k_f}{c_{p,f} \Delta x} \right)_e, \quad a_W = (\rho_f v_f)_w + \left( \frac{\epsilon_b k_f}{c_{p,f} \Delta x} \right)_w, \quad a_P^0 = \frac{\Delta x}{\Delta t} \epsilon_b \rho_{f,P}^0 \quad (3.4.61)$$

$$S_C = h S (T_s - T_{f,ref}), \quad \tilde{R}_C = r_f, \quad S_P = \frac{h S}{\bar{c}_{p,f}} \quad (3.4.62)$$

$$a_P = a_E + a_W + a_P^0 + (S_P + \tilde{R}_C) \Delta x \quad (3.4.63)$$

Boundary conditions:

$x = A$  :

$$\begin{aligned} a_P h_{f,P} &= a_E h_{f,E} + a_A h_{f,A} + a_P^0 h_{f,P}^0 + S_C \Delta x \\ a_A &= (\rho_f v_f)_A + 2 \left( \frac{\epsilon_b k_f}{c_{p,f} \Delta x} \right)_A \\ a_P &= a_E + a_A + a_P^0 + (S_P + \tilde{R}_C) \Delta x \end{aligned} \quad (3.4.64)$$

$x = B$  :

$$\begin{aligned} a_P h_{f,P} &= a_W h_{f,W} + a_P^0 h_{f,P}^0 + S_C \Delta x \\ a_E &= 0 \\ a_P &= a_W + a_P^0 + (S_P + \tilde{R}_C) \Delta x \end{aligned} \quad (3.4.65)$$

## 3.5 Overall algorithm

The numerical formulation of the mathematical model has been presented so far. For effective implementation of discretized equations into a computer program, it is necessary to specify an overall algorithm with the order of execution of particular steps. The overall algorithm is outlined in the figure 3.2.

After initialization of all variables by values defined in a data file outside the program, the time loop starts with the first time step. In the beginning of each time step the coefficients  $a_p^0$  must be calculated from the values obtained in the previous time step, i.e.  $a_p^0$ 's are given by initialized values loaded in the very beginning. Each time step is iterated until the convergence is reached. The coefficients from process rate equations are recalculated in each iteration before the discretized governing equations are solved.

It should be pointed out that when checking the convergence the number of iterations also may indicate divergence in a sense. It can happen that each pair of two successive solutions may not change as less as it is required for getting the convergence, so the iteration loop might become an endless cycle. Thus it is good practice to state a maximum number per a time step which, when exceeded, stops the iteration loop. If such a case arises, the time step can be shorten and the algorithm can continue from the time where it has been interrupted. If the time step becomes too small, the computer run is stopped and the method is said to have not converged. After a successful time step the solution is saved. Due to the length of the time step which often happens to be as low as a thousandth of second, it is not necessary to save solution after each time step. Instead, it can be saved in some representative times.

## 3.6 Program implementation

To get some results and make conclusions about suitability of the mathematical model the overall algorithm has been implemented in the MATLAB code. This environment is very suitable for numerical simulations. It provides a vast of built-in functions on numerical algorithms as they are known from the theory. Via the M-files one can write a code according to his needs and let it build by the MATLAB compiler (or better to say builder) to an executable.

Programming of numerical algorithms in MATLAB becomes even more practical when the obtained solution does not seem to be correct in accordance to the expectations. Final tuning can be done by the MATLAB debugger, in which all variable values can be watched during the execution by setting breakpoints in the code, and changed to another value to see if the new values produce the expected result. A lot of inspiration on effective implementation of numerical methods can be found in [21], [22].

### 3.6.1 Data and M-file organization

The program consists of several M-files and a data file where all values necessary for the initialization are defined. The main M-file from which the others are called is `grateCombustMain.m`. The time loop is represented by the `while` cycle and it runs until it reaches the end of the given time interval. During this loop, several other M-files are executed in the order that corresponds with the overall algorithm shown in the figure 3.2. The script `coeff.m` contains definitions of all coefficients needed for evaluating the

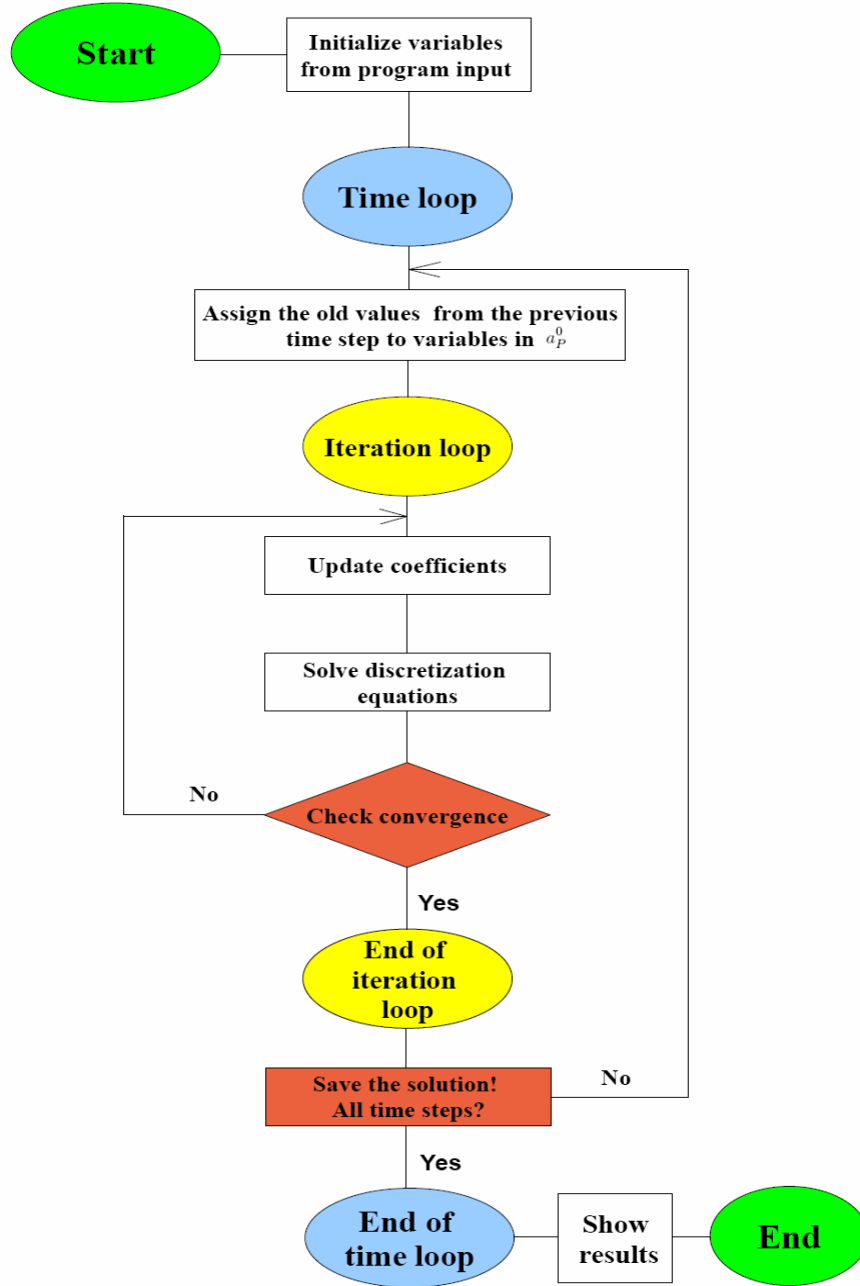


Figure 3.2: Overall algorithm

discretized equations. These are solved by the function `solve.m` which accepts diffusion, convective, and source terms as well as the type of boundary values, the values themselves, previous time and iteration solutions, and the spatial step  $\Delta x$  as its arguments and returns the new values of the variable for which it has been called. Inside the function, coefficients  $a_i$  from (3.2.19) are calculated. Since the domain is discretized into a hundred of cells at most, the matrix of the system of equations is not that large not to effectively utilize the Gauss elimination method (GEM) using the sparse representation of the matrix.

The Gauss-Seidel method has also been tried, but due to very slow convergence it has been commented out and replaced by GEM. The function `solve.m` has also been tested in such stationary convection-diffusion problems for which the analytical solutions are easy to find, so the results have been compared to make sure there is no mistake.

The time step is controlled and modified in a simple way whenever a larger (more than 10) or fewer number of iterations is needed to obtain the time solution. This control is very important during the solution, since it helps the program adapt to sometimes very fast changing values of variables.

### 3.6.2 Program tuning and simulation results

It can hardly be expected that the first or second program run will be without complications. Even after tens of simulations it has shown some difficulties which have been hard to smooth away. The resulting MATLAB program is not fully functional to be used for prediction of straw combustion. However, it has proved all results mentioned in articles on this topic, namely the strong dependence of processes on the mass transfer coefficient and convective heat transfer coefficient.

Two different scenarios have been used to simulate combustion. The first one has modeled the situation where no radiation heat source has been used and the biomass has been heated and dried up only by air preheated to the temperature 900 K, at which the devolatilization starts to be very significant. The second scenario has taken into account the heat source which has been placed in the middle of the fuel bed in order not to violate the boundary conditions as mentioned in 2.5.2. These situations are analysed in detail in the following.

#### Scenario 1: preheated air without heat source

The purpose of this simulation is to examine the moisture evaporation and devolatilization caused by hot air flow, and possibly state the reasons of resulting values. As it has been mentioned, one of the most influential coefficient is the mass transfer coefficient  $k_d$ . The relation for the mass transfer coefficient taken from [5] results in large values of the coefficient which causes excessive moisture evaporation (unrealistic cooling) and after several time steps the program breaks down with a message of matrix singularity. The reason of such behaviour has not been identified, but an arbitrary smaller constant value of  $k_f$  (several orders of magnitude) does not produce the same behaviour.

The figure 3.3 shows distributions of temperatures in both fluid and solid phases after 1000 s of the simulation run. It may be observed that the solid temperature at the bottom of the bed reaches above the fluid temperature as the simulation has been stopped at the moment of the onset of char combustion. Along the bed the both temperatures decrease due to heat consumed in fuel drying and devolatilization. The progress of devolatilization may be observed in the figure 3.4 where it is seen that significant amount of volatiles have been released from the first few control volumes of the fixed bed. The impact of the arbitrarily chosen value of  $k_d$  which controls the rates of evaporation and char combustion may be seen from the low drop of the mass. It is important to note that the mass transfer coefficient, and by extension the evaporation and char combustion rates should depend on the solid temperature as well as on instantaneous composition. This requirement is not satisfied in the present model, because the expression for  $k_d$  taken from the literature [5]



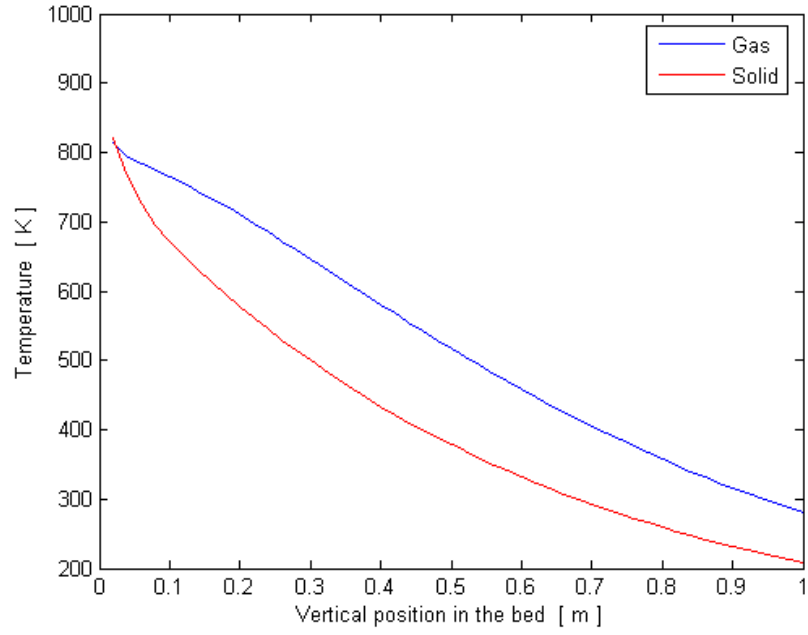


Figure 3.3: Temperature distributions

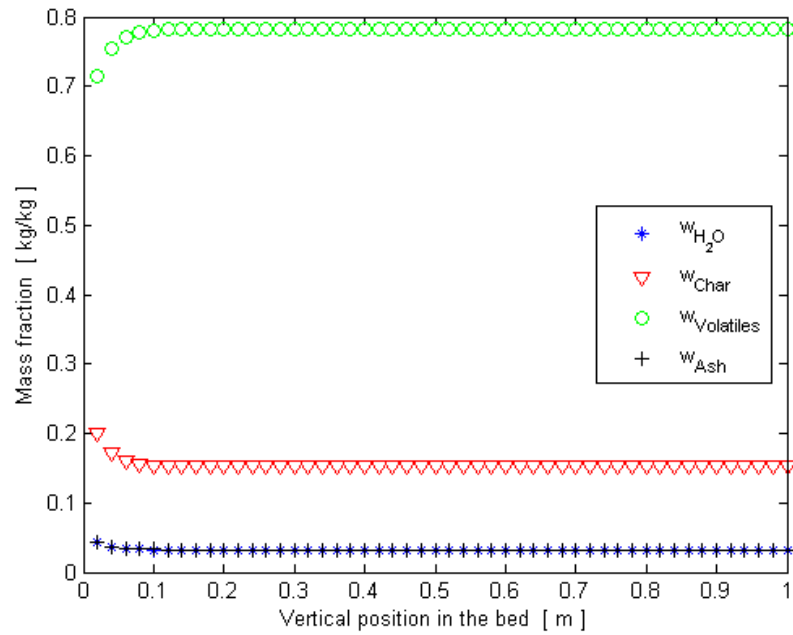


Figure 3.4: Mass fractions in solid

has proven to contain an unknown error. The constant value used instead does not reflect the dependence of the coefficient on the solid temperature. To illustrate the composition of the gas phase, figure 3.5 is displayed, showing the gas composition along the bed height.

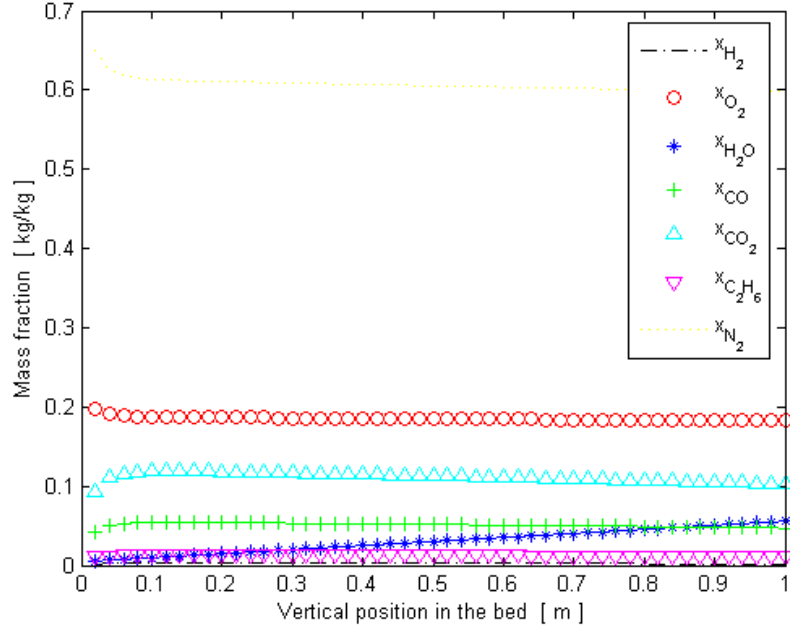


Figure 3.5: Mass fractions of gas species

## Scenario 2: radiation heat source in the middle of the bed

This simulation is done in order to validate the model in a situation similar to the practical intended use. For the sake of simplicity it has been decided to keep the same boundary conditions in all simulations which in turn prevents the possibility to heat the solid bed by radiation from the top. Therefore the heat source was placed in the middle of the fuel bed (arbitrarily). This change provides for simple implementation while leading to a very similar physical situation. The reasons for doing that have been explained in the section (2.5.2).

The same facts as discussed in the scenario 1 regarding the mass transfer coefficient and subsequently evaporation and char combustion rates apply for the second scenario as well. Namely, the heat release by the char combustion process and heats consumed in drying and devolatilization of the fuel are not in harmony which is reflected by the mass loss rate history in figure 3.6. The figure 3.6 shows that the mass loss is far from being smooth and contains a number of very sharp peaks. The individual peaks correspond to the instance of intense char oxidation in individual control volumes. This again demonstrates the imbalance of the three main processes (moisture evaporation, devolatilization, char oxidation).

The figure 3.7 displays the instantaneous composition of the solid in vertical cross-section of the bed. The most curious feature in the figure is the profile of the water content. The peak of water mass fraction coincides with the position of the heat source which is very hard to explain by physical reasoning. Furthermore, the region of devolatilized fuel has very sharp boundaries which neither seems to be realistic. The reason for this strange behaviour must be sought in the expressions used for process rates within the bed.

The last two figures show the temperatures of solid and gas phases and mass fractions

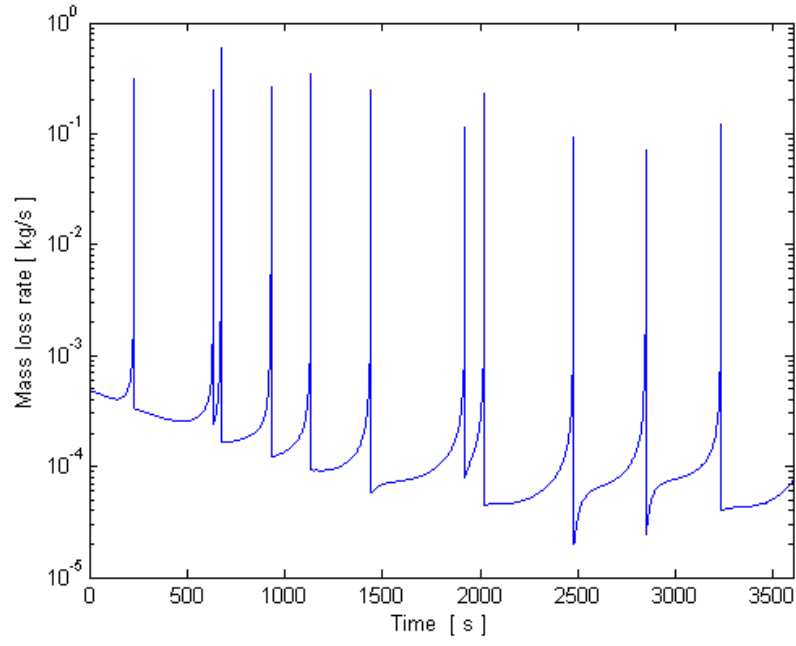


Figure 3.6: Mass loss rates

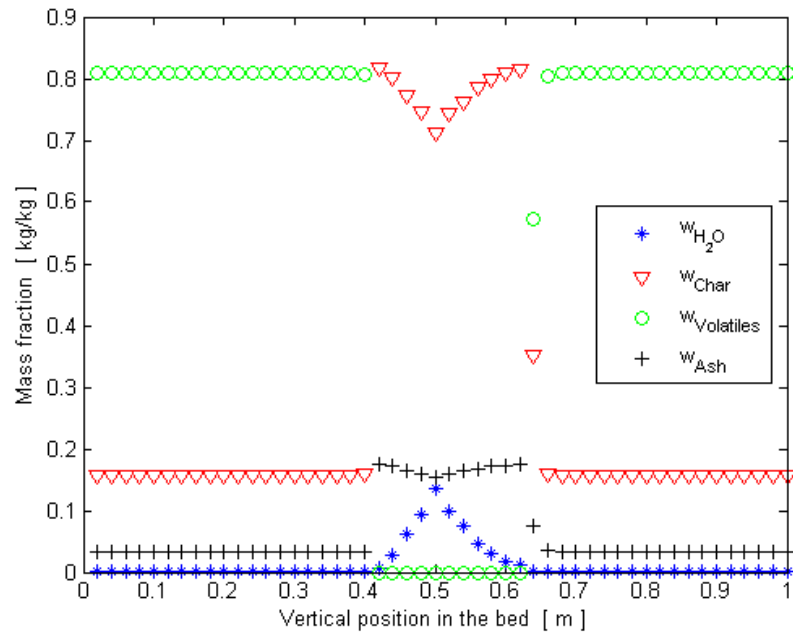


Figure 3.7: Mass fractions in solid

of the gas phase.

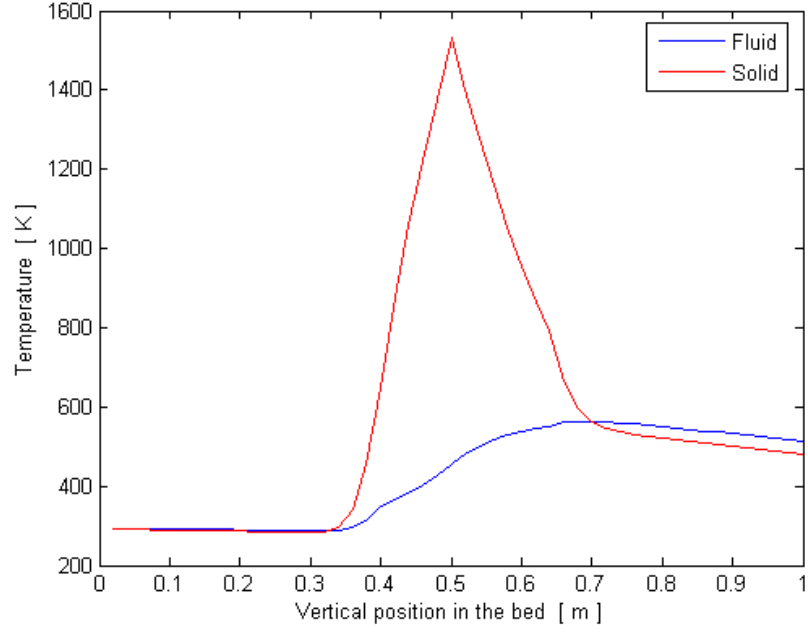


Figure 3.8: Gas and solid temperatures

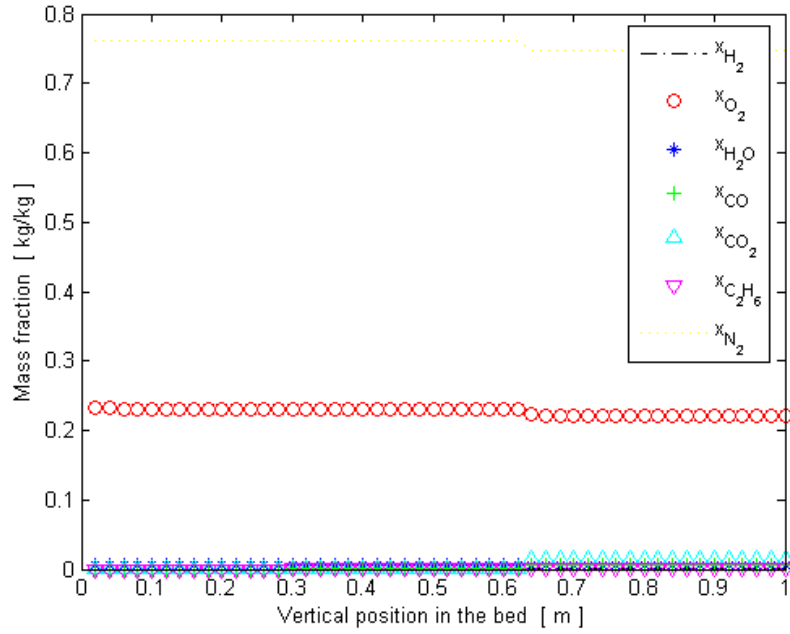


Figure 3.9: Mass fractions of gas species

### 3.7 Summary

Discretization of the general transport equation has been presented. This result has been applied to the governing equations, so the numerical model has been described. The

overall algorithm has been proposed and two different scenario simulations have been presented with discussion on the results.

## Chapter 4

### Conclusion and future work

The thesis has explained the significance of one-dimensional modelling of grate combustion of solid fuels. A detailed description of a mathematical model has been given. The partial differential equations governing the overall process have been discretized by the finite volume method and the resulting numerical model has been implemented in the MATLAB code. Numerous simulations have been done, and the results of two scenarios have been shown. These results have proved the strong dependence of combustion simulations accuracy on the quality of data inputs and mainly on proper relations that describe processes occurring in the bed. Some mistakes that have accidentally appeared in literature have been found out and corrected.

However, there are doubts about some relations which deserve more future attention, investigation and testing using the software. This should be the subject of future work and studies. Also there is much to do with developing the computer program to serve as a reliable tool for prediction of biomass combustion.

# Bibliography

- [1] Hájek J.: *Modelování s využitím CFD - I*, studijní materiál pro 2. stupeň magisterského studia, Vysoké učení technické v Brně, 2007
- [2] *FLUENT 6.2.16 Users Guide*, Fluent, Inc., Lebanon, 2006
- [3] Kær S.K.: *Numerical investigation of ash deposition in straw-fired boilers*, Ph.D. thesis, Aalborg University, Denmark, 2001
- [4] Miltner M., Miltner A., Makaruk A., Harasek M., Friedl A.: *CFD simulation of solid biomass combustor: modelling approaches for the reduction of emissions and maximisation of the thermal efficiency*, 17th International Congress of Chemical and Process Engineering, Prague, 2006
- [5] van der Lans R.P., Pedersen L.T., Jensen A., Glarborg P., Dam-Johansen K.: *Modelling and experiments of straw combustion in a grate furnace*, Biomass & Bioenergy, Vol. 19, pp. 199-208, 2000
- [6] Zhou H., Jensen A.D., Glarborg P., Jensen P.A., Kavaliauskas A.: *Numerical modelling of straw combustion in a fixed bed*, Fuel, Vol. 84, pp. 389-403, 2005
- [7] Yang Y.B., Sharifi V.N., Swithenbank J.: *Effect of air flow rate and fuel moisture on the burning behaviours of biomass and simulated municipal solid wastes in packed beds*, Fuel, Vol. 83, pp. 1553-1562, 2004
- [8] Goerner K., Klasen T.: *Modelling, simulation and validation of the solid biomass combustion in different plants*, Progress in Computational Fluid Dynamics, Vol. 6, Nos. 4/5, 2006
- [9] Recman M.: *Mathematical models of great combustion of solid fuels*, Master thesis, Brno University of Technology, Czech Republic, 2007
- [10] Yang Y.B.: *Effect of fuel properties on biomass combustion. Part II. Modelling approach - identification of the controlling factors*, Fuel, Vol. 84, pp. 2116-2130, 2005
- [11] Murthy J.Y.: *Numerical methods in heat, mass and momentum transfer* [online], [cit. 2008-17-01]. URL: <<http://widget.ecn.purdue.edu/~jmurthy/me608/main.pdf>>
- [12] Lukáčová M.: *Mathematical methods in fluid dynamics*, Vysoké učení technické v Brně, 2003
- [13] Pavelek M. a kolektiv: *Termomechanika*, Vysoké učení technické v Brně, 2003

- [14] Massman W.J.: *A review of the molecular diffusivities of  $H_2O$ ,  $CO_2$ ,  $CH_4$ ,  $CO$ ,  $O_3$ ,  $SO_2$ ,  $NH_3$ ,  $N_2O$ ,  $NO$ , and  $NO_2$  in air,  $O_2$ , and  $N_2$  near STP*, Atmospheric Environment, Vol. 32, pp. 1111-1127, 1998
- [15] *The Engineering Toolbox* [online], [cit. 2008-20-05].  
 URL: <[http://www.engineeringtoolbox.com/thermal-conductivity-d\\_429.html](http://www.engineeringtoolbox.com/thermal-conductivity-d_429.html)>  
 URL: <[http://www.engineeringtoolbox.com/air-properties-d\\_156.html](http://www.engineeringtoolbox.com/air-properties-d_156.html)>
- [16] Čermák L.: *Numerické metody II*, Vysoké učení technické v Brně, 2004
- [17] Hirsch C.: *Numerical Computation of Internal and External Flows - Volume 1: Fundamentals of Numerical Discretization*, John Wiley & Sons, 1989
- [18] Hirsch C.: *Numerical Computation of Internal and External Flows - Volume 2: Computational Methods for Inviscid and Viscous Flows*, John Wiley & Sons, 1990
- [19] Patankar S.V.: *Numerical Heat Transfer and Fluid Flow*, Taylor & Francis, 1980
- [20] Horová I., Zelinka J.: *Numerické metody*, Masarykova univerzita, 2004
- [21] MATLAB Help: *User's guide*, version 7, The MathWorks, Massachusetts, USA, 2004
- [22] Yang W.Y., Cao W., Chung T., Morris J.: *Applied Numerical Methods Using MATLAB*, John Wiley & Sons, 2004



# Nomenclature and acronyms

$c_{p,f}$	specific heat capacity of the gas phase [ $\text{J}\cdot\text{kg}^{-1}\text{K}^{-1}$ ]
$c_{p,s}$	specific heat capacity of the solid phase [ $\text{J}\cdot\text{kg}^{-1}\text{K}^{-1}$ ]
$\bar{c}_{p,f}$	mean specific heat capacity of the gas phase [ $\text{J}\cdot\text{kg}^{-1}\text{K}^{-1}$ ]
$\bar{c}_{p,s}$	mean specific heat capacity of the solid phase [ $\text{J}\cdot\text{kg}^{-1}\text{K}^{-1}$ ]
$C_{w,f}$	concentration of moisture in the gas phase [ $\text{kg}/\text{m}^3$ ]
$C_{w,s}$	concentration of moisture at the solid surface [ $\text{kg}/\text{m}^3$ ]
$d_{ex}$	external diameter of straw [m]
$D_{a,eff}$	effective axial dissipation coefficient [ $\text{m}^2\cdot\text{s}$ ]
$D_i$	molecular diffusion coefficient of species i [ $\text{m}^2\cdot\text{s}$ ]
$F$	flux (in discretization equation)
$h$	gas-solid heat transfer coefficient [ $\text{W}\cdot\text{K}^{-1}\text{m}^{-2}$ ]
$h_b$	bed height [m]
$h_f$	gas phase specific enthalpy [ $\text{J}/\text{kg}$ ]
$h_s$	solid phase specific enthalpy [ $\text{J}/\text{kg}$ ]
$k_c$	rate constant of char oxidation [ $\text{s}^{-1}\text{Pa}^{-1}\text{m}^{-3}$ ]
$k_d$	mass transfer coefficient [m/s]
$k_{eff}$	effective thermal conductivity [ $\text{W}\cdot\text{m}^{-1}\text{K}^{-1}$ ]
$k_{eff,0}$	thermal conductivity for no fluid flow [ $\text{W}\cdot\text{m}^{-1}\text{K}^{-1}$ ]
$k_f$	gas thermal conductivity [ $\text{W}\cdot\text{m}^{-1}\text{K}^{-1}$ ]
$k_o$	rate constant of char overall reaction [ $\text{s}^{-1}\text{m}^{-3}$ ]
$k_{vol}$	rate constant of devolatilization [ $\text{s}^{-1}$ ]
$\dot{m}$	mass flow rate [ $\text{kg}/\text{s}$ ]
$m_{ash}$	mass of ash [kg]
$m_{char}$	mass of char [kg]
$m_{vol}$	mass of volatiles [kg]
$M_C$	molar mass of carbon [ $\text{kg}/\text{mol}$ ]
$M_{O_2}$	molar mass of oxygen [ $\text{kg}/\text{mol}$ ]
$p$	gas pressure [Pa]
$r$	specific gas constant [ $\text{J}\cdot\text{kg}^{-1}\text{K}^{-1}$ ]
$p_{O_2}$	oxygen partial pressure [Pa]
$Pe$	Peclet number [-]
$Pr$	Prandtl number [-]
$Q_{H_2O}$	vaporization heat loss [ $\text{W}/\text{m}^3$ ]
$Q_r$	radiation heat source [ $\text{W}/\text{m}^3$ ]
$Q_s$	heat gain due to the char combustion [ $\text{W}/\text{m}^3$ ]
$r_c$	reaction rate of char oxidation [ $\text{kg}\cdot\text{s}^{-1}\text{m}^{-3}$ ]
$r_f$	conversion rate from solid to gas [ $\text{kg}\cdot\text{s}^{-1}\text{m}^{-3}$ ]
$r_{char}$	overall char reaction rate [ $\text{kg}\cdot\text{s}^{-1}\text{m}^{-3}$ ]
$r_{ext}$	external radius of the hollow straw [m]
$r_{H_2O}$	rate of moisture release [ $\text{kg}\cdot\text{s}^{-1}\text{m}^{-3}$ ]
$r_{in}$	internal radius of the hollow straw [m]
$r_{O_2}$	oxygen reaction rate [ $\text{kg}\cdot\text{s}^{-1}\text{m}^{-3}$ ]
$r_{vol}$	rate of devolatilization [ $\text{kg}\cdot\text{s}^{-1}\text{m}^{-3}$ ]

$r_{CO}$	carbon monoxide reaction rate [ $\text{kg}\cdot\text{s}^{-1} \text{ m}^{-3}$ ]
$r_{CO_2}$	$\text{CO}_2$ reaction rate [ $\text{kg}\cdot\text{s}^{-1} \text{ m}^{-3}$ ]
$r_{CO_2,c}$	rate of $\text{CO}_2$ production due to the char combustion [ $\text{kg}\cdot\text{s}^{-1} \text{ m}^{-3}$ ]
$R$	ideal gas constant [ $\text{J}\cdot\text{mol}^{-1}\text{K}^{-1}$ ]
$Re$	Reynolds number [-]
$S$	particle surface area per unit volume [ $\text{m}^2/\text{m}^3$ ]
$S_\phi$	source term (in discretization equation)
$t$	time [s]
$T_f$	gas (fluid) temperature [K]
$T_s$	solid temperature [K]
$\Delta t$	time step [t]
$u$	velocity (in discretization equation)
$v_f$	gas velocity [ $\text{m}\cdot\text{s}^{-1}$ ]
$V$	volume [ $\text{m}^3$ ]
$V_f$	gas volume [ $\text{m}^3$ ]
$V_s$	solid volume [ $\text{m}^3$ ]
$W_{char}$	molecular weight of carbon [ $\text{kg}/\text{mol}$ ]
$x$	spatial coordinate [m]
$X_i$	gas phase species [ $\text{kg}/\text{kg}$ ]
$\Delta x$	space step [m]
$\gamma_i$	mass fraction of volatile i [ $\text{kg}/\text{kg}$ ]
$\Gamma$	diffusion coefficient
$\epsilon_b$	bed porosity [-]
$\phi$	an unknown function
$\nu_f$	gas viscosity [ $\text{Pa}\cdot\text{s}$ ]
$\rho_{char}$	density of char in straw wall [ $\text{kg}/\text{m}^3$ ]
$\rho_f$	gas density [ $\text{kg}/\text{m}^3$ ]
$\rho_s$	bulk density of straw [ $\text{kg}/\text{m}^3$ ]
$\rho_{straw}$	density of the straw wall [ $\text{kg}/\text{m}^3$ ]

CFD: Computational Fluid Dynamics

FDM: Finite Difference Method

FEM: Finite Element Method

FVM: Finite Volume Method

GEM: Gauss Elimination Method

PDE: Partial Differential Equation

UDF: User Defined Function